

1.3- μm and 10-Gbps tunable DBR-LD for low-cost application of WDM-based mobile front haul networks

SU HWAN OH,^{*} OH KEE KWON, KI SOO KIM, AND CHUL WOOK LEE

Photonics Convergence Components Research Group, Electronics and Telecommunications Research Institute, 218 Gajeongno, Yuseong-gu, Daejeon, South Korea

**osh@etri.re.kr*

Abstract: We report a 1.3- μm and 10-Gbps tunable distributed Bragg reflector laser diode (DBR-LD) for the low-cost application of a wavelength division multiplex based mobile front-haul network. The device consists of gain, phase control, and DBR sections, implemented using a butt-coupling method through a monolithic integration and through the introduction of an etched mesa planar buried hetero-structure in a waveguide structure. From the work, a 560- μm long DBR-LD with a 220- μm long micro-heater DBR section has a threshold current of $10\text{ mA} \pm 1\text{ mA}$ and a tuning range of more than 15 nm within a heater injection current of $\sim 100\text{ mA}$. Spectral and dynamic tests for this LD show 16 channels spaced a wavelength grid of 0.8 nm with a side mode suppression ratio of greater 40 dB and clear eye openings with a dynamic extinction ratio of over 5.4 dB at an operating current of 60 mA.

© 2019 Optical Society of America under the terms of the [OSA Open Access Publishing Agreement](#)

1. Introduction

Wavelength tunable lasers have achieved considerable interests in next-generation broadband backhaul and radio access networks based on wavelength division multiplexing (WDM) systems [1–3]. In particular, they have been under review as light sources in WDM-based mobile front-haul networks [4,5] because tunable lasers capable of supporting multiple sub-channel wavelengths within individual CWDM channel bands are greatly needed. These light sources should also be cost-effective and compact, as well as have a uniform performance over all sub-channels.

A distributed Bragg reflector-laser diode (DBR-LD) is one of the most promising light sources for such networks owing to its compact size, easy construction, and good long-term reliability, as compared with other DBR structures such as a sampled grating [6,7] and digital super-mode [8]. Various types of DBR-LDs with single grating mirror have been reported for high speed operation [9] and wide tuning range [10]. We recently demonstrated the use of widely tunable DBR-LDs with dual tuning elements [11], where a tuning range of approximately 19 nm was obtained using only heater tuning. For the waveguide structure of the LD, two types of structures, a RWG and a planar buried hetero-structure (PBH) were used, and we also applied both to multi-channel 10-Gbps distributed feedback-laser diode arrays (DFB-LDAs) [12–14].

From the viewpoint of the manufacturing process of DBR-LD, butt-coupled regrowth and benzo-cyclobutene (BCB) processes are of paramount importance. In previous studies [15,16], we developed an optimized butt-coupled regrowth method, which can improve the uniformity and reproducibility. In this letter, we describe the fabrication of a three-section DBR-LD using a heater tuning method and show both 10Gbps operation at 1.3 μm and wide tuning of more than 15 nm. To reduce the operating current and parasitic capacitances, a PBH is introduced, the region containing the active/passive core and the current blocking structures is etched in a mesa form (i.e., an etched mesa PBH), and BCB island regions are fabricated under the pad metal. To obtain 16 channels spaced at a wavelength interval of 0.8 nm within the effective CWDM band

(i.e., a tuning range of 13 nm (± 6.5 nm)), the phase control section is inserted into the DBR-LD for fine control of the lasing wavelength. The etched mesa PBH and the BCB island structures are implemented and optimized for a 10-Gbps operation.

2. Design and fabrication

A schematic structure of the DBR-LD is shown in Figs. 1(a) and 1(b). This laser has three sections, namely, gain, phase control, and DBR sections. The length of each section was designed to be 250, 50, and 220 μm , respectively. The lasing wavelength was tuned using a heater metal implemented on the waveguide of the DBR section. Isolation regions were inserted between the metal lines of each section for electrical isolation. The width and depth of the isolation region were 20 and 0.5 μm , respectively. The grating was patterned on the undoped InGaAsP (bandgap wavelength $\lambda_g \cong 1.2$ μm) under a passive waveguide layer, as shown in Fig. 1(a). A passive waveguide layer was butt-coupled with an active layer. The cross-section of the active region and passive waveguide were fabricated into a PBH achieve a lower power consumption and better beam quality output, and these PBH regions were then etched out to reduce the parasitic capacitance of the DBR-LD, as shown in Fig. 1(b).

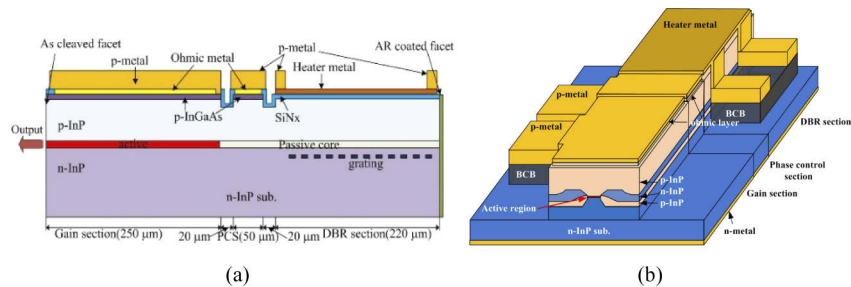


Fig. 1. (a) Layer structures of the three-section DBR-LD composed of gain, phase control, and DBR sections and (b) a schematic configuration of the DBR-LD.

These DBR-LDs were fabricated using a five-step MOCVD growth procedures. During the first growth step, a n-InP buffer layer, a 30 nm thick un(doped)-InGaAsP ($\lambda_g \cong 1.2$ μm) grating layer, and a un-InP layer were grown in sequence. The grating was formed in the DBR section using an e-beam lithography method, and its period and duty cycle were designed to satisfy the conditions for a lasing wavelength of nearly 1.31 μm and a coupling coefficient of approximately 30 cm^{-1} [17]. The length of the grating was implemented as 200 μm and shifted 20 μm toward the DBR facet for the fabricated DBR-LDs. During the second growth step, an un-InP layer, an active layer, and a p-InP cap layer were grown. The active layer consists of a strained multiple-quantum well (MQW) structure with double separate confinement hetero-structure (SCH) layers, and has seven 6nm-thick compressive-strained InGaAsP ($\lambda_g \cong 1.38$ μm) wells, six 8nm-thick tensile-strained InGaAsP ($\lambda_g \cong 1.0$ μm) barriers, and two SCH layers with 35nm-thick InGaAsP ($\lambda_g \cong 1.05$ μm and $\lambda_g \cong 1.08$ μm , respectively).

As for the butt-coupling regrowth, a 15- μm wide and 250- μm long SiO_2 mask pattern for the active region was aligned along the [110] direction on the second growth wafer using the photolithography process. In addition, a p-InP cap layer and an active layer were etched out using the reactive ion etching (RIE) process, and were then additionally wet-etched to remove the RIE residuals. The third growth step for butt-coupling was conducted through the growth of a 0.25- μm thick un-GaInAsP ($\lambda_g \cong 1.12$ μm) waveguide layer and a 0.1- μm thick InP layer. A surface image and a cross-sectional SEM image of the butt-coupled region are shown in Figs. 2(a) and 2(b), respectively. Figures 2(a) and 2(b) show surface images after the regrowth of the butt-coupled region and an SEM image of the tilted regrown region, respectively. The

butt-coupled interface was tilted 10-degrees with respect to the [110] direction to reduce the internal reflection of the DBR-LD, and the interface shape was different from that previously used [15,16] without an irregular regrowth pattern at the butt-coupled interface. For this study, we used a different wet etchant, namely, an HBr-based solution, because of the composition of the barrier layer (InGaAsP, $\lambda_g \cong 1.0 \mu\text{m}$) of the MQW layer, which was not etched through a selective wet etchant. In addition, the SEM image shows a good butt-coupled shape without any visible defects in the regrown tilted interface region, which is essential for the fabrication of an integrated laser with uniformity and a high coupling efficiency.

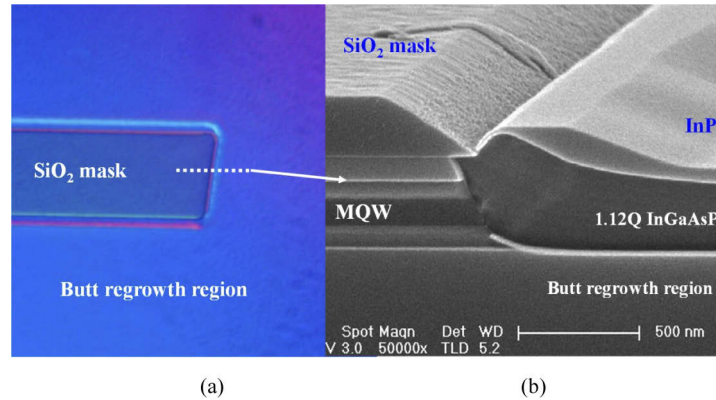


Fig. 2. (a) A microscopic image of the butt-coupled region and (b) a cross-sectional SEM image of the butt-coupled interface region.

For the formation of the p-n-p current blocking, 1.5- μm wide SiNx mask stripes lined up along the $\langle 011 \rangle$ direction were patterned, and these stripes were then etched using the RIE and wet etching processes such that the width of the active layer could be adjusted to approximately 1 μm . After the formation of the mesa structure, the fourth growth step for the p-n-p current blocking was applied. A p-InP clad layer and a p-InGaAs ohmic layer were grown during the final growth step.

Figures 3(a) and 3(b) show SEM images of the gain and DBR sections on the fabricated three-section DBR-LD after BCB curing and the Au plating process, respectively. In this waveguide structure, the width and depth of the etched mesa PBH region were fabricated to be 8 and 5 μm , respectively. BCB islands on one side of the etched mesa were formed using selective wet etching and the BCB process. Because the depth of the etched mesa PBH is approximately 3 μm higher than that of the etched mesa alone, a planarization process using BCB is difficult to apply [18]. Therefore, we used a photoresist BCB and the distance between the BCB pattern and etched mesa PBH was designed to be 10 μm . Therefore, the BCB formed does not appear to have an irregular pattern such as an over-shape in the region of the etched mesa PBH, and achieves a good formation, as indicated in Figs. 3(a) and 3(b).

A Ti/Pt/Au electrode was formed as a p-type ohmic contact of the gain section, and a Cr/Au electrode was used as the heater metal of the DBR section, the thickness of which was 30/200 nm. The width and length of the heater metal were designed to be 5 and 220 μm , respectively. On the bottom of the wafer, a Cr/Au electrode was formed as an n-type ohmic contact.

The facet of the gain section was as-cleaved and that of the DBR section was anti-reflection (AR) coated using two-layer SiO₂/TiO₂ [12]. A reflectivity of less than 1% was obtained for the operating wavelength range. To measure the dynamic characteristics, the chip was bonded onto a copper-tungsten (CuW) metal optical bench (MOB) with a high-speed flexible printed circuit board (FPCB). The structure and performance of the module are described in [12].

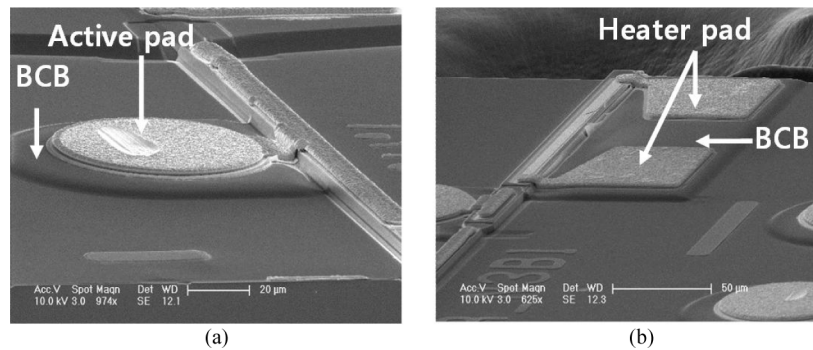


Fig. 3. An SEM image of the fabricated three-section DBR-LD, (a) an SEM image of the gain section, and (b) an SEM image of the DBR section.

3. Results and discussion

Figure 4(a) shows the light versus injection current and applied voltage (L-I-V) characteristics of the fabricated DBR-LDs at an operating temperature of 25 °C. The maximum output power was 35 mW under CW operation. The threshold current of the DBR-LDs is within the range of 10 ± 1 mA, and the slope efficiency appears to be 0.24 mW/mA at an injection current of 50 mA. In the L-I curves, kinks resulting from the longitudinal mode-hopping are observed at a high injection current range of more than 100 mA. Figure 3(b) shows the measured output spectra of the DBR-LDs at injection currents of 50 and 100 mA. As the current increases, the lasing wavelength is red shifted by 0.76 nm. The side mode suppression ratio (SMSR) of the DBR-LDs was larger than 40 dB for the two injection.

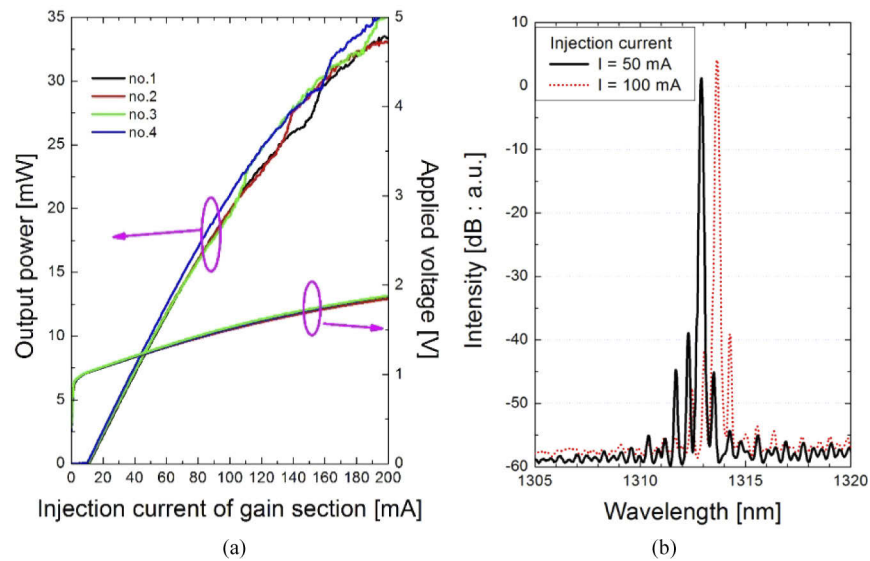


Fig. 4. (a) L-I-V characteristics of the fabricated DBR-LDs as a function of the injection current, and (b) output spectra of the DBR-LD. The resolution of the optical spectrum analyzer is 0.01 nm.

Figure 5 shows the lasing wavelength and SMSR characteristics with respect to the heater current of the DBR region. During this experiment, the injection current of the gain section was

fixed at 60 mA and the heater current of the DBR section was increased to 90 mA with a step of 1 mA. The resistance of the heater metal was measured to be approximately 62Ω . When the heater current was 90 mA, the applied power was approximately 0.5 W. When the heater current increases, the lasing wavelength is shifted toward a longer wavelength side with some mode jumps. Near a mode jump, the lasing wavelength is abruptly changed to the next mode of a longer wavelength. The SMSR is more than 35 dB except in the mode-jump regions. For the heater tuning, the tuning range has a parabolic shape with an increase in the current according to the linear relation between the heat-induced refractive index change (i.e., wavelength tuning) and electrical power, as shown in Fig. 4. The lasing wavelength was changed from 1,312 to 1,327 nm, and as a result, the wavelength tuning range of approximately 15 nm was obtained within a heater current of 90 mA.

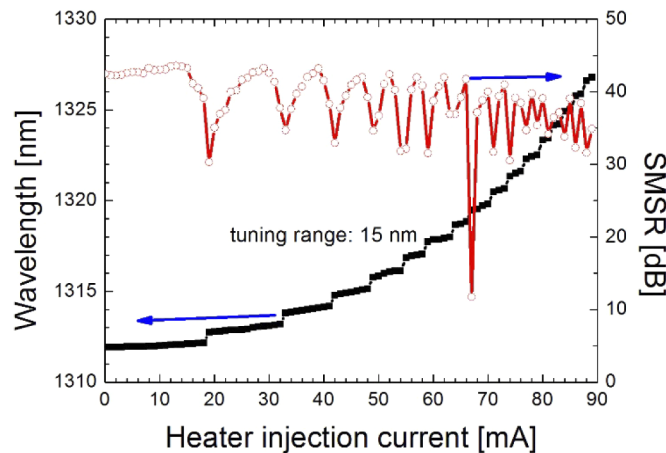


Fig. 5. Wavelength tuning and SMSR characteristics of three-section DBR-LD with only a heater current injection applied into the DBR section.

Figure 6 shows the superimposed CW spectra of the 16 channels spaced at a wavelength interval of 0.8 nm within the 13 nm tuning range (i.e., 1,312 to 1,325 nm). These spectra were obtained through the simultaneous control of the heater current in the DBR section and current in the phase control section (i.e., phase current) at a gain current of 60 mA. In this study, the phase current and heater current were varied within the range of 0 to 20 mA, and 0 to 80 mA, respectively. The phase current allowed all 16 channels to be aligned precisely at the 0.8 nm interval with an SMSR of more than 40 dB. The fiber-coupled output power was more than 2 dBm under CW operation, and the variation in output power was approximately 1 dB.

The measured eye diagram at the back-to-back (BTB) for the 16 channels is shown in Fig. 7. The DBR-LD is directly modulated for 10 Gbps with a pseudo random bit sequence (PRBS) of $2^{31}-1$ (non-return-to-zero) with a bias current of 60 mA and an amplitude of 40 mA (± 20 mA). The eye patterns are clearly opened with extinction ratios (ERs) of more than 5.4 dB. From these results, we confirmed that the fabricated DBR-LD was successfully operated at over 10 Gbps under direct modulation.

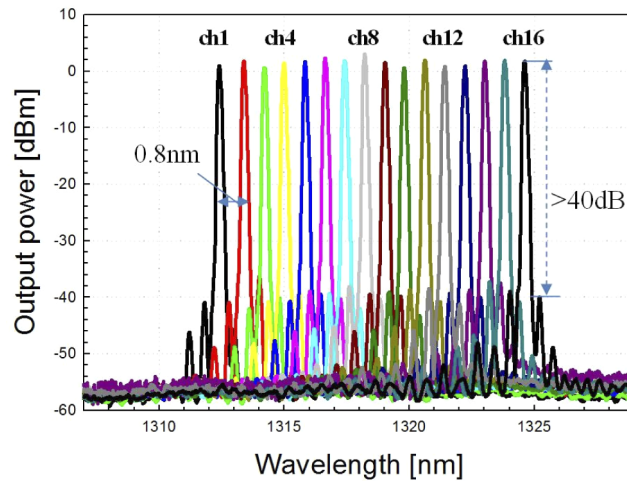


Fig. 6. Fiber-coupled output spectra of 16 channels with a 100GHz spacing and SMSR characteristics.

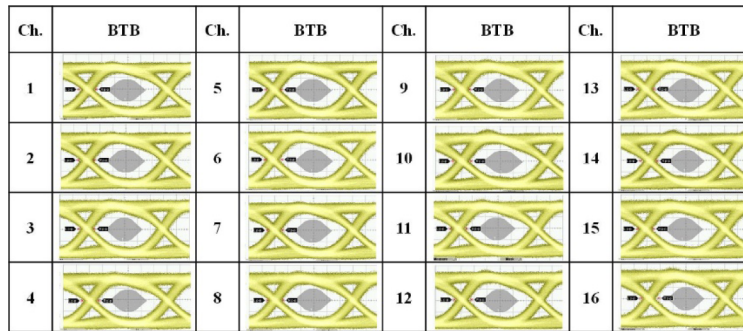


Fig. 7. Measured eye diagram at the back-to-back for all channels.

4. Summary

We developed a tunable three-section DBR-LD within a 15 nm tuning range using a heater tuning method. Sixteen channels spaced in a wavelength grid of 0.8 nm with an SMSR of more than 40 dB were obtained using a simultaneous control of the heater current and the phase current. A three-section DBR-LD was fabricated using a PBH for a low operating current, and the structures of the etched mesa and BCB islands were optimized to obtain a direct modulation of 10 Gbps. The threshold currents of the fabricated LDs were 10 ± 1 mA. The device shows clear eye patterns at a BTB with an ER of over 5.4 dB at a low operating current of 60 mA for the entire tuning range. These results confirm that the proposed three-section DBR-LD is useful for application in direct modulation devices at 10 Gbps.

Funding

Institute for Information and Communications Technology Promotion and the Government of Korea (MSIT) (Grant # 2018-0-01041).

Acknowledgment

This work was supported by Institute for Information and Communications Technology Promotion (IITP) grant funded by the Korea government (MSIT) (2018-01041, Development of low-cost tunable laser for mobile front-haul network).

References

1. J. Zhu, A. Wonfor, S. H. Lee, S. Pachnicke, M. Lawin, R. V. Penty, J.-P. Elbers, R. Cush, M. J. Wale, and I. H. White, "Athermal colorless C-band optical transmitter system for passive optical networks," *J. Lightwave Technol.* **32**(22), 4253–4260 (2014).
2. A. Pizzinat, P. Chanclou, F. Saliou, and T. Diallo, "Things you should know about fronthaul," *J. Lightwave Technol.* **33**(5), 1077–1083 (2015).
3. I. A. Alimi, A. L. Teixeira, and P. P. Monterio, "Toward an efficient C-RAN optical fronthaul for the future networks: a tutorial on technologies requirements, challenges, and solutions," *IEEE Commun. Surv. Tutorials* **20**(1), 708–769 (2018).
4. J. Shin, S. Hong, J. Y. Lim, S. Cho, H. Y. Rhy, and G. Y. Yi, "CWDM network with dual sub-channel interface for mobile fronthaul and backhaul deployment," in *Proc. 16th Int. Conf. Adv. Commun. Technol. paper*, pp. 1009–1102, (2014).
5. TTA Standard for Multichannel CWDM Applications with Multi Sub-channel Optical Interface, TTAE.KO-03.0022/R2, 2018.
6. L. A. Coldren, "Monolithic tunable diode lasers," *IEEE J. Sel. Top. Quantum Electron.* **6**(6), 988–999 (2000).
7. S. H. Oh, H. Ko, K. S. Kim, J. M. Lee, C. W. Lee, O. K. Kwon, S. Park, and M. H. Park, "Fabrication of Butt-coupled SGDBR laser integrated with semiconductor optical amplifier having a lateral tapered waveguide," *ETRI J* **27**(5), 551–556 (2005).
8. A. J. Ward, D. J. Robbins, G. Busico, E. Barton, L. Ponnampalam, J. P. Duck, N. D. Whitbread, P. Williams, D. C. J. Reid, A. C. Carter, and M. J. Wale, "Widely tunable DS-DBR laser with monolithically integrated SOA: Design and performance," *IEEE J. Sel. Top. Quantum Electron.* **11**(1), 149–156 (2005).
9. T. Kameda, H. Mori, S. Onuki, T. Kikugawa, Y. Takahashi, F. Tsuchiya, and H. Nagai, "A DBR laser employing passive-section heaters, with 10.8 nm tuning range and 1.6 MHz linewidth," *IEEE Photonics Technol. Lett.* **5**(6), 608–610 (1993).
10. K. Shinoda, T. Kitatani, Mo. Aoki, M. Mukaikubo, K. Uchida, and K. Uomi, "1.3-um InGaAlAs short-cavity DBR lasers for uncooled 10-Gb/s operation with low drive current," *IEEE Photonics Technol. Lett.* **18**(22), 2383–2385 (2006).
11. O. K. Kwon, C. W. Lee, K. S. Kim, S. H. Oh, and Y. A. Leem, "Proposal of novel structure for wide wavelength tuning in distributed Bragg reflector laser diode with single grating mirror," *Opt. Express* **26**(22), 28704–28712 (2018).
12. O. K. Kwon, Y. A. Leem, Y. T. Han, C. W. Lee, K. S. Kim, and S. H. Oh, "A 10 × 10 Gb/s DFB laser diode array fabricated using a SAG technique," *Opt. Express* **22**(8), 9073–9079 (2014).
13. O. K. Kwon, Y. A. Leem, C. W. Lee, K. S. Kim, H. M. Park, and E. S. Nam, "Simple technique for evaluating dimensional and compositional changes in selective-area-grown MQW laser diode," *Opt. Express* **22**(19), 23694–23703 (2014).
14. S. H. Oh, O. K. Kwon, K. S. Kim, Y. T. Han, C. W. Lee, Y. A. Leem, J. W. Shin, and E. S. Nam, "A multi-channel etched-mesa PBH DFB laser array using a SAG technique," *IEEE Photonics Technol. Lett.* **27**(24), 2567–2570 (2015).
15. S. H. Oh, C. W. Lee, J. M. Lee, K. S. Kim, H. Ko, S. Park, and M. H. Park, "The design and the fabrication of monolithically integrated GaInAsP MQW laser with butt-coupled waveguide," *IEEE Photonics Technol. Lett.* **15**(10), 1339–1341 (2003).
16. S. H. Oh, J.-M. Lee, K. S. Kim, C.-W. Lee, H. Ko, S. Park, and M.-H. Park, "Fabrication of wavelength tunable butt-coupled sampled grating DBR lasers using planar buried heterostructure," *IEEE Photonics Technol. Lett.* **15**(12), 1680–1682 (2003).
17. O. K. Kwon, Y. A. Leem, D. H. Lee, C. W. Lee, Y. S. Baek, and Y. C. Chung, "Effects of asymmetric grating structures of output efficiency and single longitudinal mode operation in $\lambda/4$ -shifted DFB laser," *IEEE J. Quantum Electron.* **47**(9), 1185–1194 (2011).
18. W. Kobayashi, N. Fujiwara, T. Yamanaka, T. Tadokoro, M. Arai, K. Tsusuki, and F. Kano, "Full C-band 10-Gb/s 40-km SMF transmission of InGaAlAs electroabsorption modulator," *J. Lightwave Technol.* **28**(20), 3012–3018 (2010).